Science Advances
AAAS

Supplementary Materials for

Control of striatal circuit development by the chromatin regulator *Zswim6*

Kyuhyun Choi *et al.*

Corresponding author: Marc V. Fuccillo, fuccillo@pennmedicine.upenn.edu;
Kyuhyun Choi, kyuhyun@hallym.ac.kr

Sci. Adv. **11**, eadq6663 (2025)
DOI: 10.1126/sciadv.adq6663

This PDF file includes:

Supplementary Figures

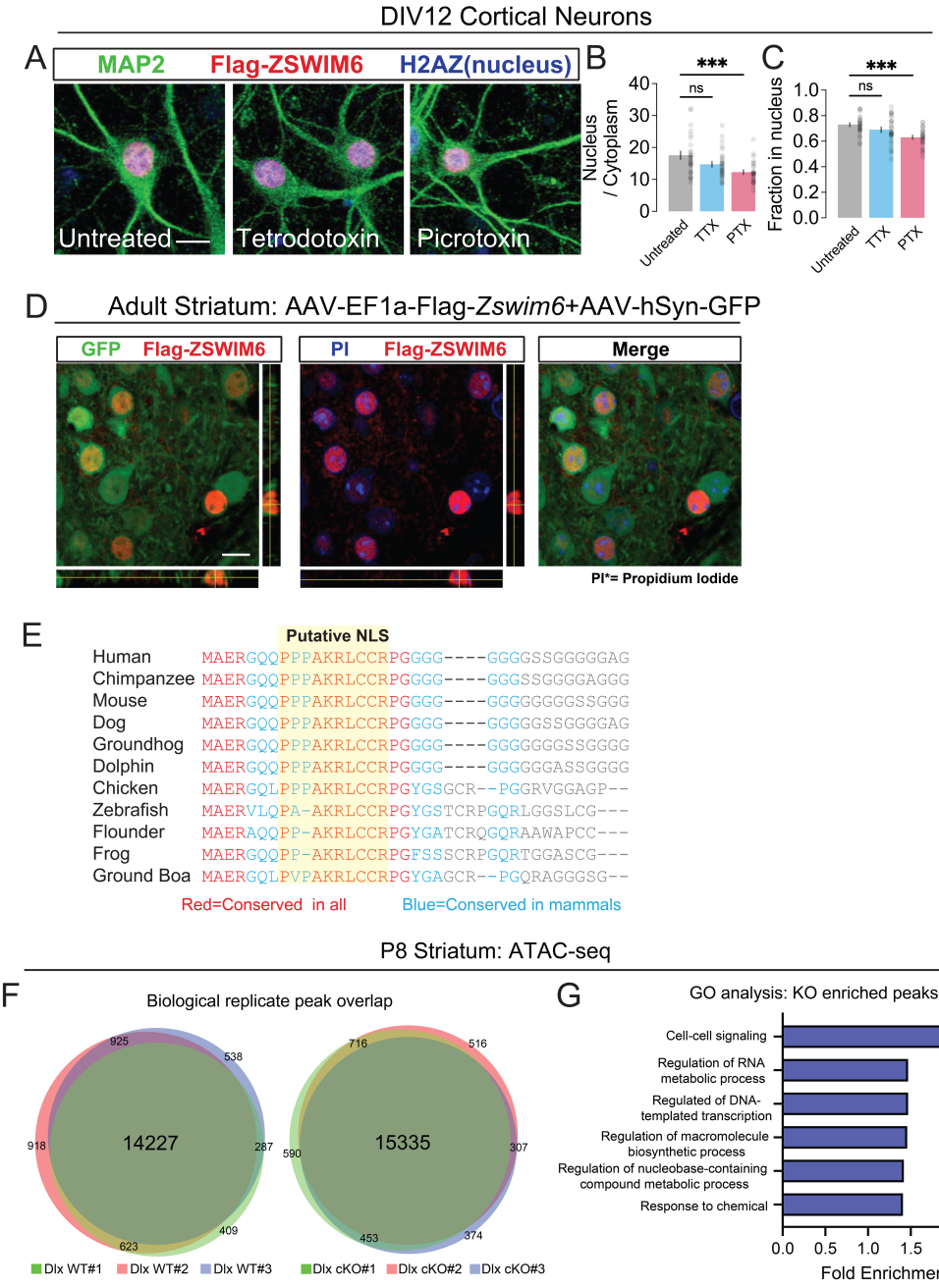

Figure S1: Nuclear localization and chromatin regulation by ZSWIM6. Related to Figure 1.

(A) Representative images of DIV12 neurons transduced with AAV-Ef1α-Flag-Zswim6 (red) and immunostained for MAP2 (green) to label cell morphology and H2AZ to label nuclei (blue). Cultures were treated with the indicated reagents for 2 hours. Scale bar, 10 μm. (B) Summary data of mean Flag-ZSWIM6 fluorescence intensity (nucleus/cytoplasm ratio) in cells treated with the indicated reagents. (n= 3 cultures for each experimental condition, Untreated n= 27 cells, TTX n=29 cells, PTX n=27 cells, One-way ANOVA, $F(2, 80) = 8.230$, ***p=0.0006, Tukey's post hoc, Untreated-TTX p=0.0762; Untreated-PTX ***p=0.0003). (C) Quantification of the fraction of Flag-ZSWIM6 intensity localized to the nucleus in cells treated with the indicated reagents (n= 3 cultures for each experimental condition, Untreated n= 27 cells, TTX n=29 cells, PTX n=27 cells, One-way ANOVA, $F(2,80) = 8.306$, ***p=0.0002, Tukey's post hoc, Untreated-TTX p=0.1887; ****Untreated-PTX p=0.0001). (D) Representative maximum projections of confocal stacks demonstrating the relationship between Flag-ZSWIM6, cell-filling GFP, and the nuclear marker propidium iodide in striatum, following co-injection of AAV-hSyn-GFP and AAV-Ef1α-Flag-Zswim6. Orthogonal views confirm nuclear localization of ZSWIM6 in the axial plane (scale bar, 10 μm). (E) Bioinformatics-based search of a well-conserved predicted nuclear localization sequence (NLS) across multiple species. (F) Overlap of peaks between Dlx-WT/cKO biological replicates demonstrating that the vast majority of peaks are shared between replicates. (G) significantly enriched gene ontology (GO) categories within the 583 TSS regions with ≥1.5-fold increase in reads per million in Dlx-cKO vs Dlx-WT striatum.

A

Animal ID	# nuclei
Dlx WT #1	7514
Dlx WT #2	5104
Dlx WT #3	5659
Dlx WT #4	4480
Dlx cKO #1	5186
Dlx cKO #2	4737
Dlx cKO #3	7326
Dlx cKO #4	5726

B

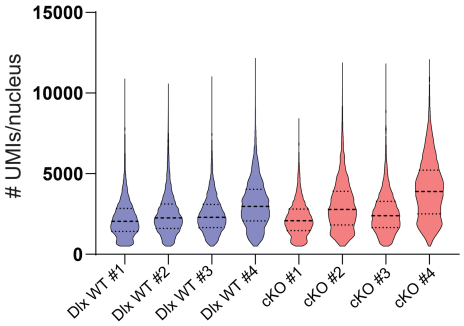

C

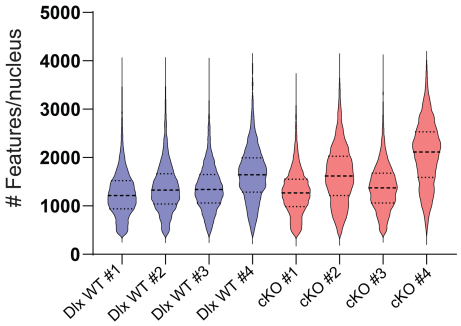

D

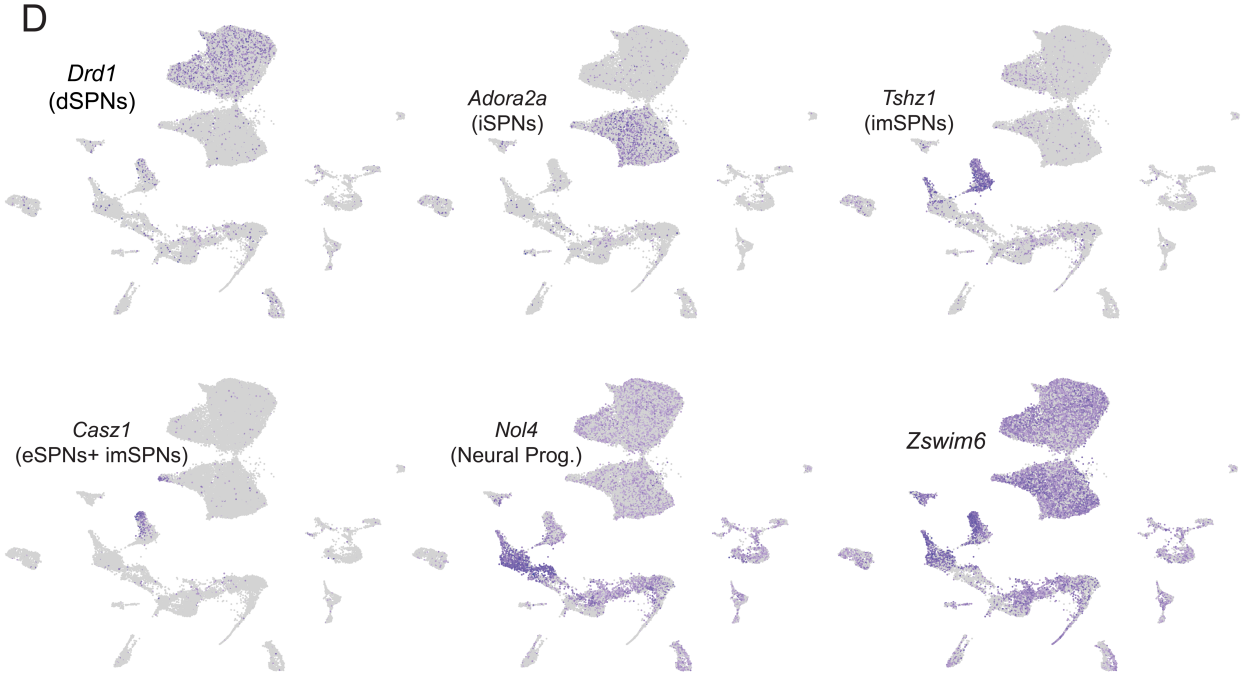

E

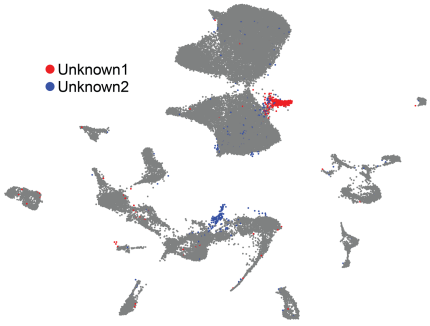

F

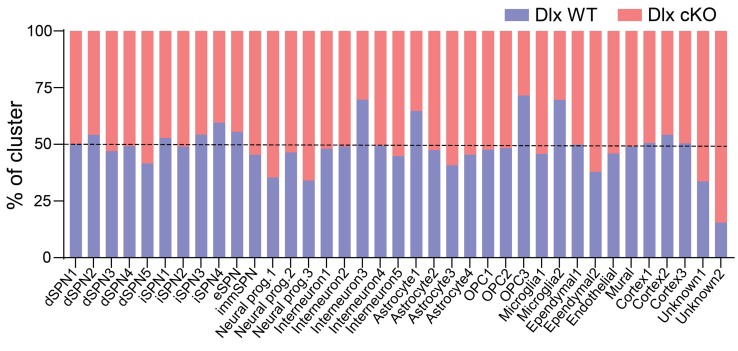

Figure S2: snRNA-seq sample and Seurat cluster information. Related to Figure 2.

(A) Number of nuclei (pre-filtered to remove doublets) in each of the 8 animals included in the snRNA-seq experiment. (B) Number of unique molecular identifiers (UMIs) per nucleus in each experimental sample (violin plots indicate median, 25th and 75th quartiles). (C) Number of identified features (genes) per nucleus in each experimental sample (D) Seurat-generated "Feature plots", displaying expression levels of selected cell markers (purple) on the UMAP plot displayed in Fig. 2. (E) Two clusters corresponding to unidentified cell types show in UMAP space. (F) Percentage of Dlx-WT/cKO nuclei in each Seurat cluster. Dashed line indicates 50%. Violin plots indicate median, 25th and 75th quartiles.

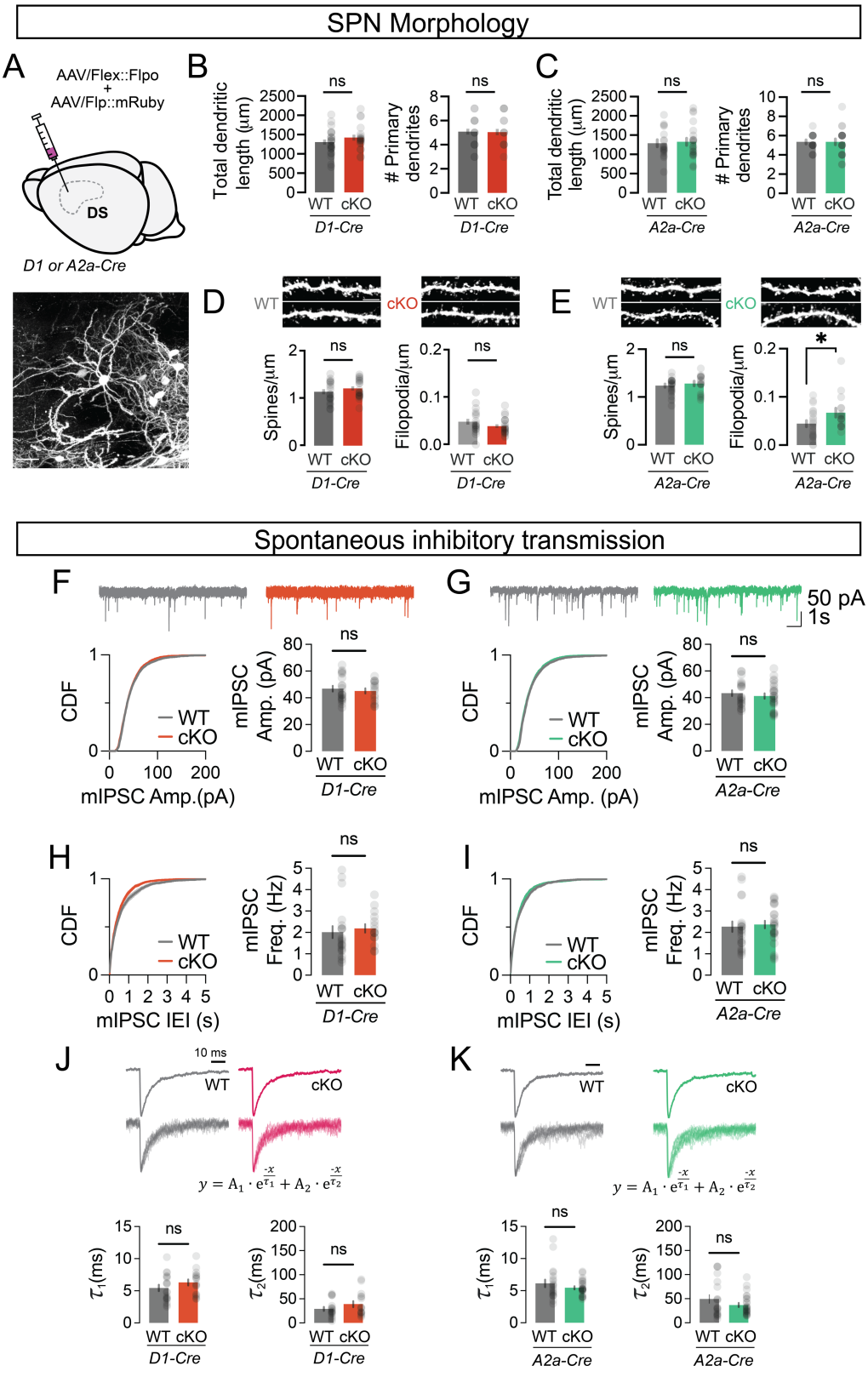
SPN Morphology
A
AAV/Flex::Flpo
+
AAV/Flp::mRuby
DS
D1 or A2a-Cre
B
Total dendritic length (µm)
Primary dendrites
ns
WT cKO
D1-Cre
C
A2a-Cre
D
WT
cKO
Spines/µm
Filopodia/µm
E
*
Spontaneous inhibitory transmission
F
G
50 pA
1s
CDF
mIPSC Amp.(pA)
mIPSC Amp. (pA)
mIPSC Amp. (pA)
H
I
mIPSC Freq. (Hz)
mIPSC IEI (s)
J
K
10 ms
$y = A_1 \cdot e^{\frac{-x}{\tau_1}} + A_2 \cdot e^{\frac{-x}{\tau_2}}$
τ_1(ms)
τ_2(ms)

Figure S3: Neuronal morphology and inhibitory synaptic transmission onto SPNs were not significantly altered by *Zswim6* knockout. Related to Figure 3.

(A) Schematic of dual virus injection strategy to achieve sparse labeling of Cre-expressing SPNs (top). Representative image of an iSPN expressing mRuby following the injection strategy above (bottom). Scale bar, 30 μm. (B) Quantification of total dendritic length (left) and number of primary dendrites (right) in D1-WT/ cKO SPNs (n= 3/3 animals, D1-WT/cKO n= 24/19 cells. Dendritic length, p=0.2552; primary dendrite number, p=0.9315, *t*-test). (C) Quantification of total dendritic length (left) and number of primary dendrites (right) in A2A-WT/cKO SPNs (n= 3/3 animals, A2A-WT/cKO n= 17/22 cells. Dendritic length, p=0.7647; primary dendrite number, p=0.9781, *t*-test). (D) Quantification of dendrite spine density (left) and filopodia density in D1-WT and D1-cKO neurons (n= 3/3 animals, D1-WT/cKO n= 18/20 cells. Spine density, p=0.3271; filopodia density, p=0.1988, *t*-test). (E) Quantification of dendrite spine density (left) and filopodia density in A2A-WT and A2A-cKO neurons (n= 3/3 animals, A2A-WT/cKO n= 22/16 cells. Spine density, p=0.4454; filopodia density, *p=0.0428, *t*-test). Scale bars in (D-E), 5 μm. (F) Representative mIPSC traces from both D1-WT/cKO (top) neurons. Scale bar, 1s, 50pA. Cumulative distribution function graph of mIPSC amplitudes (bottom-left) and comparison of average mIPSC amplitudes (bottom-right) between D1-WT/cKO neurons (n = 20/15 cells from 4/4 animals; p = 0.5948, *t*-test). (G) Similar to (F), but for *A*2A-WT/cKO (n= 20/24 cells from 4/5 animals, p=0.4620, *t*-test). (H) Cumulative distribution function graph of mIPSC inter-event interval (left) and comparison of events frequencies (right) between D1-WT and D1-cKO neurons (n= 20/15 cells from 4/4 animals, p=0.6364, *t*-test). (I) Similar to (H), but for A2A-WT/cKO (n= 20/24 cells from 4/5 animals, p=0.7296, *t*-test). (J) Averaged and scaled superimposed traces of mIPSCs from D1-WT/cKO(top) neurons. Comparison of τ1 and τ 2 decay constants obtained from fitting mIPSC traces to a double exponential function (bottom) (n= 19/15 cells from 4/4 animals, τ1 p=0.3151, τ2 p=0.2435 *t*-test). k) Similar to (J), but for A2A-WT/cKO (n= 20/24 cells from 4/5 animals, τ1 p=0.2669, τ2 p=0.1831, *t*-test). Data are presented as mean ± SEM. Each shaded dot represents data from an individual experiment, unless otherwise noted.

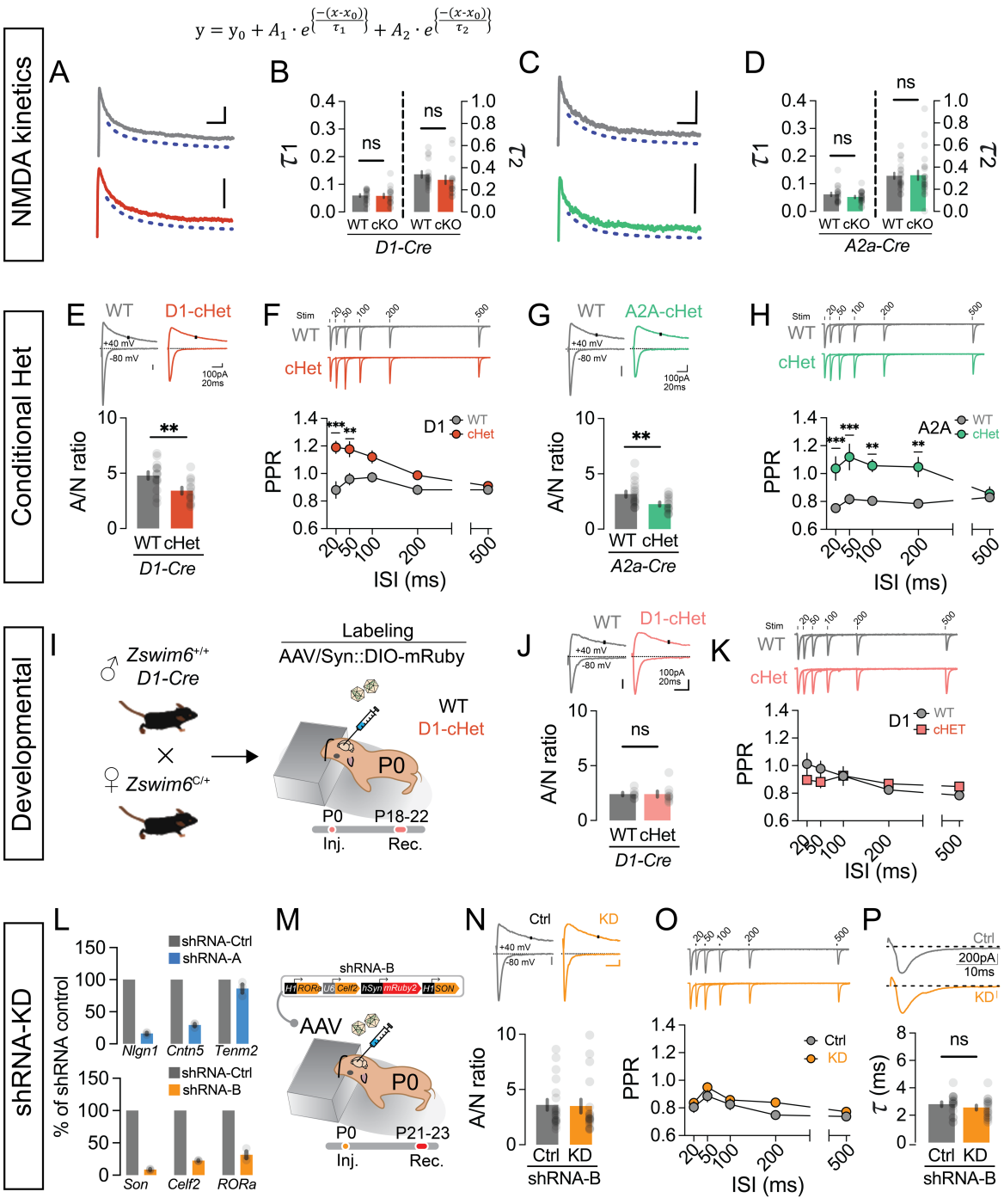
NMDA kinetics
Conditional Het
Developmental
shRNA-KD
$y = y_0 + A_1 \cdot e^{\{-(x-x_0)/\tau_1\}} + A_2 \cdot e^{\{-(x-x_0)/\tau_2\}}$
A
B
C
D
ns
WT cKO
D1-Cre
A2a-Cre
E
WT
D1-cHet
A2A-cHet
cHet
A/N ratio
WT cHet
F
G
H
PPR
ISI (ms)
D1
A2A
I
Zswim6+/+
D1-Cre
Zswim6C/+
Labeling
AAV/Syn::DIO-mRuby
P0
P0 P18-22
Inj.
Rec.
J
K
L
shRNA-Ctrl
shRNA-A
shRNA-B
% of shRNA control
Nlgn1
Cntn5
Tenm2
Son
Celf2
RORa
M
shRNA-B
AAV
P0 P21-23
N
Ctrl
KD
O
P
τ (ms)

Figure S4: Examination of NMDAR function, *Zswim6* gene dosage effects and analysis of dysregulated genes downstream of *Zswim6* disruption. Related to Figure 4.

(A) Representative traces at +40 mV holding potential for NMDA currents are presented for D1-WT/cKO (bottom) neurons. (B) Bar graphs display the decay constants (τ1 and τ2) of NMDA components derived from both D1-WT/cKO animals. The fitting was performed using a double exponential function. (n=19/17 cells from 5/5 animals, τ1 p=0.8732; τ2 p=0.3026, *t*-test). Scale bar, 50 ms 100 pA. Solid line represents the raw trace, while the blue-dotted line represents the model inferred trace. C-D) Similar to (A), but for A2A-WT/cKO (n=20/23 cells from 5/5 animals, τ1 p=0.1994, τ2 p=0.9126, *t*-test). (E) Representative traces of evoked EPSCs from D1-WT/cHet neurons obtained with cells clamped at +40 mV and -80 mV in order to determine AMPA/NMDA ratio (top). Summary data of AMPA/NMDA ratio in D1-WT and D1-cHet neurons (bottom, n= 15/13 cells from 3/4 animals, **p=0.0050, *t*-test). (F) Representative traces of evoked EPSCs D1-WT/cHet neurons obtained during paired-pulse protocol (top). Summary data of paired pulse ratio in D1-WT and D1-cHet neurons (bottom, n= 17/20 cells from 3/4 animals, RM-2way ANOVA, ISI $F(4,140)=11.65$, ***p= 3.417×10^{-8}, Genotype $F(1,35)=15.12$, ***p= 4.309×10^{-4}, Interaction $F(4,140)=5.822$, **p=0.002). (G) Similar to (E), but for A2A-WT/cHet (n= 18/15 cells from 5/3 animals, **p=0.0082, *t*-test). (H) Similar to (F), but for A2A-WT/cHet (bottom, n= 19/15 cells from 5/3 animals, RM-2way ANOVA, ISI $F(4, 128)=3.535$, **p=0.0088, Genotype $F(1,32) = 17.53$, **p=0002, Interaction $F(4,128) = 3.899$, **p=0.005). (I) An illustration of the experimental strategy to evaluate early age knockout. AAV is injected into neonatal WT and *Zswim6*-cHet pups to selectively label knockdown cells, with subsequent synaptic measurements taken at P18-22. (J) Representative traces of evoked EPSCs from D1-WT/cHet neurons during early development. Recordings were obtained with cells voltage-clamped at +40 mV and -80 mV to determine the AMPA/NMDA ratio. (top). Summary data of AMPA/NMDA ratio in D1-WT/cHet neurons (bottom, n= 7/9 cells from 4/4 animals, p=0.9964, *t*-test). (K) Representative traces of evoked EPSCs D1-WT/cHet neurons obtained during paired-pulse protocol (top). Summary data of paired pulse ratio in D1-WT/cHet neurons (bottom, n= 17/20 cells from 3/4 animals, RM-2way ANOVA, ISI $F(4,60)=7.753$, ***p= 4.186×10^{-5}, Genotype $F(1,15)=0.2103$, p= 0.6531, Interaction $F(4,60)=3.615$, **p=0.01,). (L) qPCR validation of AAV mediated shRNA efficiency (top, shRNA-A; bottom, shRNA-B). Each data point for shRNA-A and shRNA-B groups is displayed as a percentage of expression level of the corresponding gene in shRNA-Control transduced neurons from the same batch of cultures. (M) An illustration of the shRNA-B approach. shRNA AAV vectors (*RORa, Celf2, Son*) are injected into neonatal CD1 pups to selectively knock down gene expression, with subsequent synaptic measurements taken at P21-P23. (N-P) Representative traces (top) along with a comparison of the (N) AMPA/NMDA ratio(n= 20/18 cells from 4/4 animals, p=0.8819, *t*-test) or (M) PPR (n= 20/17 cells from 4/4 animals, RM-2way ANOVA, ISI $F(4,140)=14.16$, p< 9.97×10^{-10}, shRNA $F(1,35)=1.955$, p=0.1708, Interaction $F(4,140) = 0.6908$, p=0.5995) or (P) τ (n= 20/18 cells from 4/4 animals, p=0.8819, *t*-test) between mice injected with control shRNA and mice injected with shRNA-B. Data are presented as mean ± SEM. Each shaded dot represents data from an individual experiment, unless otherwise noted. Significance from Šídák's post-hoc test for RM-2way ANOVA.

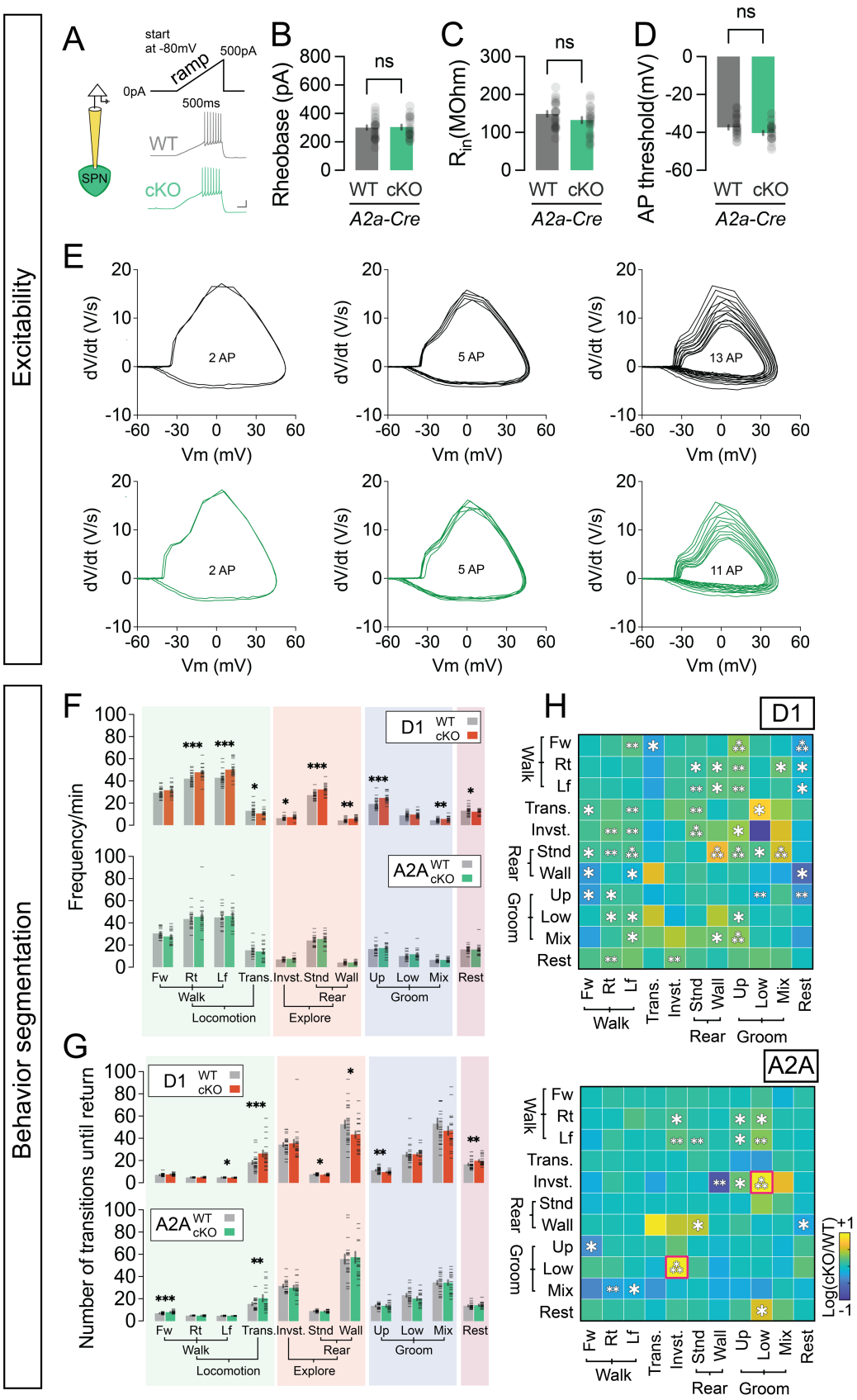
Excitability
A
start
at -80mV
ramp
500pA
0pA
500ms
WT
cKO
SPN
B
Rheobase (pA)
ns
WT cKO
A2a-Cre
C
R_in (MOhm)
ns
WT cKO
A2a-Cre
D
AP threshold(mV)
ns
WT cKO
A2a-Cre
E
dV/dt (V/s)
Vm (mV)
2 AP
5 AP
13 AP
2 AP
5 AP
11 AP
Behavior segmentation
F
Frequency/min
D1 WT cKO
A2A WT cKO
Fw Rt Lf Trans. Invst. Stnd Wall Up Low Mix Rest
Walk
Locomotion
Rear
Explore
Groom
G
Number of transitions until return
D1 WT cKO
A2A WT cKO
H
D1
A2A
Log(cKO/WT)
+1
-1

Figure S5: Additional analyses of passive membrane properties and spontaneous behavior in SPN-specific *Zswim6* cKOs. Related to Figure 5.

(A) Protocol for assessing intrinsic membrane properties and excitability in SPNs. (B) Summary data comparing rheobase between A2A-WT/cKO SPNs (n= 23/19 cells from 5/4 animals, p=0.7414, *t*-test). (C) Summary data comparing input resistance between A2A-WT/cKO SPNs (n= 23/19 cells from 5/4 animals, p=0.2210, *t*-test). (D) Summary data comparing action potential threshold between A2A-WT/cKO SPNs (n= 23/19 cells from 5/4 animals, p=0.0632, *t*-test). (E) dV/dt firing curves from A2A-WT and A2A-cKO, showing when 2, 5, and 11(13) action potentials occurred. (F) Frequency of each behavioral cluster from D1-WT/cKO (top) and A2A-WT/cKO (bottom) (bootstrap BCa test). (G) Number of transitions until return of each behavioral cluster from D1-WT/cKO (top) and A2A-WT/cKO (bottom) (bootstrap BCa test). (H) Log-scaled comparison of transition matrix ratios between WT and cKO groups. The upper panel represents the data for D1-WT/cKO mice, while the lower panel represents the data for A2A-WT/cKO mice (See Table. S1 to see detailed statistics).

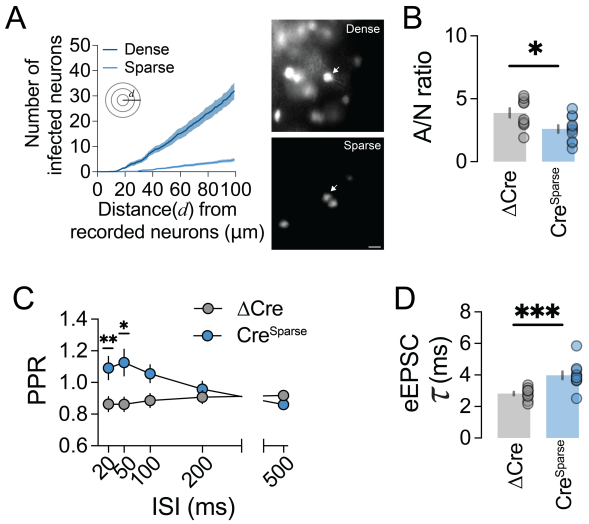

Figure S6: Sparse expression of Cre phenocopies the effects of dense Cre expression. Related to Figure 6.

(A) Cumulative frequency distribution of neuronal density expressing Cre-GFP between full titer (Dense, Figure 6) and 1/10 titer (Sparse, Figure S6) (left, mean ± SEM represented as thick line ± shaded area, n=9/14 from 3/3 animals, Repeated Two-way ANOVA, titer $F(1,21)=79.71$, ***$p=1.3574\times10^{-8}$, distance $F(99,2079)=135.81$, ***$p<1*10^{-12}$, Interaction $F(99,2079)=73.14$, ***$p<1*10^{-12}$). Captured images obtained from each viral titer configuration (right). (B) AMPA/NMDA ratio (n= 10/11 cells from 3/3 animals, $p=0.0126$, *t*-test) or (C) PPR (n= 11/8 cells, RM-2way ANOVA, $F(3.294, 55.99) = 4.844$, **$p<0.003$, Cre $F(1, 17) = 7.453$, *$p=0.014$, Interaction $F(4, 68) = 10.59$, ***$p=9.988\times10^{-9}$) or (D) τ (n= 11/11 cells, ***$p=0.0002$, *t*-test) between mice injected with ΔCre-GFP and mice injected with 1/10 Cre. Data are presented as mean ± SEM. Each shaded dot represents data from an individual experiment, unless otherwise noted. Significance from Šídák's *post-hoc* test for RM-2way ANOVA.

D1-Cre		Walk				Explore			Groom			
		Fw	Rt	Lf	Trans.	Invst.	Stand	Wall	Upper	Lower	Mix	Rest
Walk	Fw		0.057128	0.00148	0.011039	0.232821	0.11951	0.285367	2.54E-05	0.318013	0.499396	9.57E-05
	Rt	0.318975		0.209034	0.063127	0.303965	0.039788	0.033281	0.002963	0.491999	0.041596	0.049217
	Lf	0.05832	0.261537		0.156029	0.064926	0.007945	0.045609	0.001888	0.381495	0.078161	0.036995
	Trans.	0.03215	0.000403	0.009098		0.012335	0.00605	0.470485	0.050485	0.027851	0.174118	0.052394
Explore	Invst.	0.066078	0.002158	0.0055	0.058655		0.000372	0.212731	0.011493	0.127082	0.082134	0.096333
	Stand	0.049945	0.001277	0.000167	0.326951	0.133963		4.98E-06	1.24E-05	0.047325	1.33E-05	0.102919
	Wall	0.012573	0.430226	0.034437	0.110146	0.350713	0.108092		0.264108	0.160662	0.10322	0.018481
Groom	Upper	0.041737	0.033286	0.05519	0.271772	0.176613	0.07916	0.300938		0.009927	0.114958	0.002798
	Lower	0.43525	0.01174	0.012707	0.115437	0.170719	0.361425	NaN	0.049142		0.379415	0.191982
	Mix	0.371606	0.371499	0.034713	0.22405	0.12557	0.164747	0.014867	4.96E-05	0.453393		0.195372
	Rest	0.25829	0.001489	0.000162	0.368937	0.004887	0.054676	0.304564	0.11788	0.171784	0.238115	

Table S1: Detailed statistics relating to Figure S5C. p-value summary of transition matrix from *D1-Cre* mice (bootstrap test). Colored boxes indicate p-value <0.05.

A2a-Cre		Walk				Explore			Groom			
		Fw	Rt	Lf	Trans.	Invst.	Stand	Wall	Upper	Lower	Mix	Rest
Walk	Fw		0.130797	0.448155	0.287633	0.180879	0.17251	0.351838	0.271004	0.430023	0.173594	0.360051
	Rt	0.252331		0.116477	0.337334	0.045058	0.262632	0.15544	0.016488	0.030636	0.360577	0.488299
	Lf	0.008693	0.283128		0.323319	0.001594	0.003944	0.181334	0.013086	0.005141	0.336125	0.127802
	Trans.	0.355294	0.500066	0.451211		0.467864	0.172545	0.333787	0.173145	0.270263	0.311984	0.462796
Explore	Invst.	0.132157	0.167804	0.482885	0.02274		0.243102	0.004388	0.015342	2.32E-08	0.166934	0.214081
	Stand	0.163739	0.300455	0.398894	0.305323	0.474772		0.184034	0.442935	0.068391	0.09365	0.114321
	Wall	0.415894	0.44891	0.37482	0.108023	0.174096	0.014179		0.070704	0.456067	0.434431	0.030341
Groom	Upper	0.030477	0.420167	0.47161	0.465026	0.057781	0.42057	0.191815		0.158943	0.436015	0.225883
	Lower	0.184994	0.494413	0.428906	0.462397	1.25E-08	0.268921	0.120167	0.297734		0.384874	0.366721
	Mix	0.296651	0.009681	0.046175	0.110031	0.469892	0.329013	0.094009	0.175669	0.116118		0.115318
	Rest	0.090728	0.222122	0.278608	0.151896	0.099229	0.219779	0.058639	0.146402	0.047226	0.287866	

Table S1 (continued): Detailed statistics relating to Figure S5C. p-value summary of transition matrix from *A2a-Cre* mice (bootstrap test). Colored boxes indicate p-value <0.05.

Primer name	Primer sequence
*Actb*_Forward	CGCAGCCACTGTCGAGTC
*Actb*_Reverse	GTCATCCATGGCGAACTGGT
*Hprt*_Forward	AGTCCCAGCGTCGTGATTAG
*Hprt*_Reverse	TGATGGCCTCCCATCTCCTT
*Nlgn1*_Forward	CCCCATGATTGGCCCTACAG
*Nlgn1*_Reverse	TGGTTGATTTGGGTCACCAG
*Cntn5*_Forward	CATTGCCTGGGAGCCAGTAT
*Cntn5*_Reverse	GCCTCCGAAGACGTAACCAT
*Tenm2*_Forward	AAACCGAGTCACAGACCTGG
*Tenm2*_Reverse	CAGGGTGAAGTTTGTCCCTTGT
*Son*_Forward	AAAAAGTCTGGAGGAGCTACCA
*Son*_Reverse	AGGAGGTTCTTCTTCCTCTTCA
*Celf2*_Forward	ATGTTTGAGCGCACTTCTGA
*Celf2*_Reverse	TCCGTTCATCTTGTTGGCTGT
*Rora*_Forward	CGAAGAAGACACACACATCTCA
*Rora*_Reverse	CAGGAGTAGGTGGCATTGCT

Table S2: List of primer sequences used for qPCR.